Investigating Molecular Mechanisms of Calcium Signaling in Bacterial Pathogen *Pseudomonas aeruginosa*

Rendi Rogers

HONORS THESIS

Advisor: Dr. M.A. Patrauchan

Graduate Mentor: B. Kayastha

May 2018

INTRODUCTION

Pseudomonas aeruginosa is a human pathogen that causes acute and chronic infections [1] [2]. *P. aeruginosa* infections cause cellular damage and airway blockage by forming biofilms in the respiratory systems of cystic fibrosis (CF) patients. These biofilm infections are often not treatable using antibiotics [3] [4] [5]. For these reasons, *P. aeruginosa* infections are a leading cause of death in patients with CF [6] [7].

Calcium (Ca^{2+}) is a signaling ion whose regulatory role has been extensively studied in eukaryotes and shown to be essential in orchestrating many essential biological processes [8]. Abnormal cellular Ca^{2+} homeostasis is associated with multiple diseases, including pulmonary infections in CF patients, and the dysregulation of Ca^{2+} metabolism has been shown to contribute to CF pathology [9]. It has been shown to accumulate in the respiratory systems of CF patients [10]. Furthermore, Ca^{2+} plays a role in host response to bacterial infection [11].

Ca^{2+} has also been shown to influence bacterial physiology [12]-[16]. *P. aeruginosa*, among other bacteria, is able to maintain intracellular Ca^{2+} homeostasis as well as respond to Ca^{2+} in the environment [17] [18] [19]. Currently, however, the molecular mechanisms of Ca^{2+}-signaling have not been adequately studied in prokaryotes. Research in Patrauchan's lab has shown that increased levels of Ca^{2+} induce the production of several virulence factors in *P. aeruginosa*, including extracellular proteases, alginate, pyocyanin, formation of biofilm, and antibiotic resistance [20].

In order to study the molecular mechanisms regulating Ca^{2+}-induced virulence in *P. aeruginosa*, the Patrauchan lab had predicted several putative Ca^{2+}-binding proteins. The group identified the only calmodulin-like protein encoded in the *P. aeruginosa* genome, EfhP. This protein contains two canonical Ca^{2+}-binding EF-hand domains [20]. EfhP was also shown to be involved in mediating Ca^{2+}-regulated virulence and resistance in the pathogen [20]. EfhP is predicted to be one component of a Ca^{2+}-signaling network. However, its specific role in this putative network is currently unknown.

The principal goal of my research has been to elucidate the role that EfhP plays in regulating Ca^{2+}-induced virulence of *P. aeruginosa.* To achieve this goal, I aimed to: (1) purify EfhP and measure its Ca^{2+}-binding properties, (2) identify specific amino acids binding Ca^{2+} in EfhP, and (3) study the environmental factors affecting transcriptional regulation of the encoding gene, *efhP*. This knowledge is imperative for characterizing the functional role of EfhP. Considering the importance of Ca^{2+} signaling in a host, its understanding would provide an insight into the regulatory networks orchestrating virulence and interactions with a host in *P. aeruginosa*. The latter is essential for future development of novel therapeutic approaches for preventing or controlling *Pseudomonas* infections.

METHODS AND MATERIALS

Heterologous expression and purification of EfhP

The wild-type strain of *P. aeruginosa*, PAO1, was used for this study. The predicted cytoplasmic portion of *efhP*, represented in Figure 1, was cloned into the vector pET-15b, shown in Figure 2, which has ampicillin resistance for antibiotic selection as well as a TEV protease cleavage site for removal of His-tag in the purified protein.

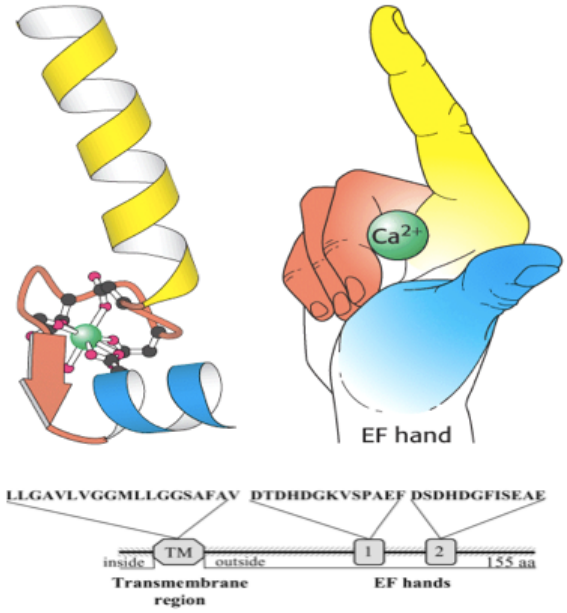

Figure 1. EfhP is a transmembrane protein with two EF-Hand domains. These domains have a helix-turn-helix structure and are known to bind Ca^{2+}.

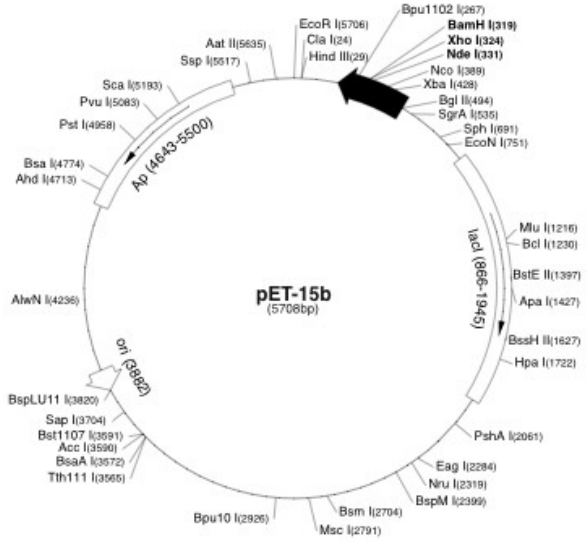

Figure 2. *efhP* was cloned into the vector pET-15b between the BamHI and NdeI restriction sites.

The soluble portion of *efhP* was amplified by PCR from the PAO1 genome using gene specific primers efhP_OM forward and efhP reverse, shown in Table 1. The amplicon was digested for 3 hours at 37°C along with the cloning vector pET15b using restriction enzymes BamHI and NdeI. *efhP* was then cloned into pSKB3 using a Quick Ligation kit (NEB). The ligation mixture was incubated at room temperature for 15 minutes. The resulting construct, named pDAV, contained *efhP* between the BamHI and NdeI restriction sites under the IPTG-inducible promoter. It was transformed by using heat-shock transformation protocol [21]. For this, the ligated vector was added to heat shock competent DH5α *E. coli* cells, kept on ice for 30 minutes, incubated at 42°C for 45 seconds, then kept on ice for an additional 10 minutes. The cells were then transferred to 1mL LB broth in a glass tube and incubated for 2 hours at 37°C. 150 µL of the cells were spread on LB agar plate with the selective antibiotic ampicillin (100µg/ml). Successful transformants were confirmed by PCR amplification followed by DNA sequencing.

For protein purification, pDAV was transformed into the expression strain DE3 *E. coli* using the heat shock protocol described above. The expression cells were grown in 50mL LB broth with 100mg/mL ampicillin at 37°C shaking overnight. 10mL of this culture was used to inoculate 1L LB broth + 100mg/mL ampicillin and incubated at 37°C shaking for approximately 3 hours. When the OD of this culture reached 0.6, 2mL of 0.5M IPTG was added to induce expression of EfhP, and the culture was grown in the same conditions for 3 additional hours. The culture was divided into four 250mL centrifuge bottles and pelleted by centrifuging at 12,000 rpm for 30 minutes. The supernatant was discarded and the cells were stored at -20°C.

For cell lysis, the frozen pellets were thawed on ice. The cells were resuspended in 50mL buffer A: 20 mM Tris, 500 mM NaCl, 10% glycerol, 20 mM Imidazole, pH 7.8. Lysozyme was added to final concentration of 0.5mg/mL. The cells were incubated on ice for 40 minutes. The lysate was sonicated 8 seconds on, 8 seconds off for 1 minute 30 seconds. The cells were centrifuged at 12,000rpm for 30 minutes at 4°C. The supernatant was collected and incubated with 4ml of Ni-NTA resin pre-equilibrated with buffer A in a 50 ml falcon tube and put on

rocker in cold room, rocking for 1 hour. Thus charged Ni-NTA resin was transferred into a 25 ml gravity flow column and washed with 100mL of pre-chilled buffer A. The protein was eluted by using 20ml buffer B (20mM Tris, 500mM NaCl, 10% glycerol, 250mM Imidazole, pH 7.8) . The eluates were collected in fractions of 1.5ml in microcentrifuge tubes. The eluates were analyzed by SDS-PAGE to confirm the presence of the purified protein with correct molecular weight.

In order to cleave off the N-terminal 6X His-tag, the eluates containing the protein were pooled together and treated with recombinant Tobacco Etch Virus (rTEV) protease in 1:40 molar ratio (TEV: protein sample). The mixture was transferred into a dialysis membrane of molecular weight cutoff value 12-14KDa and subjected to dialysis against 1L buffer: 20 mM Tris, 500 mM NaCl, 10% glycerol, pH 8.0 in the 4°C cold room overnight. To prepare for removing the cleaved His-tag fragment and His-tag rTEV, the Ni-NTA resin was washed with 50 ml buffer B and then 100 ml pure water, then 30 ml buffer A. The column was equilibrated with 30mL dialysis buffer. The dialyzed protein sample was transferred into the column and let flow through the column 3 times by gravity flow. Buffer A was used to wash out any residual His-tag cleaved protein attached to the column. Finally buffer B was used to elute all the uncleaved His-tagged protein from the column. These fractions along with the flow through were analyzed by running on a SDS-PAGE to verify the efficiency of digestion.

The digested protein was concentrated by using a spin-column with 10K MW cut-off (Millipore) to achieve 5-10 mg/ml final protein concentration. The concentrated protein was aliquoted into 50 ul in thin-wall PCR tubes and frozen by immersing the tubes into the liquid nitrogen by using a pair of forceps. All tubes were then placed into a 50 ml falcon tube with proper labels and stored at -80°C for further analyses.

Measuring EfhP Ca^{2+}-binding capabilities

ITC measurements were performed with a Nano-Isothermal Titration Calorimeter III (Calorimetry Sciences Corporation, Utah, USA). Frozen EfhP_NO_TM was thawed and quantified using Bradford assay. Briefly, Bio-Rad protein assay dye reagent concentrate was

diluted 5 times with nanopure water. Absorbance was read at 595nm by using a spectrophotometer (Thermo Scientific). HEPES buffer (20mM HEPES, 100mM NaCl, pH 7) was used to dilute the protein sample to make the concentration 100µM. A 1mM solution of Calcium chloride ($CaCl_2$) was prepared in HEPES buffer. Prior to titration, both the protien and $CaCl_2$ were centrifuged for 1 minute at 4C, 14000 rpm in a spin filter (VWR) with nylon membrane of pore size 0.2µM. A total of 1ml of this filtered protein was titrated with a total of 250µl $CaCl_2$. The titration consisted of injecting 10µl aliquots of 1mM $CaCl_2$ solution into the protein every 300 seconds. A total of 20 injections were carried out. The ITC data was analyzed using the software Bindworks (supplied with Nano-Isothermal Titration Calorimeter III). The amount of heat released per addition of the titrant was fitted to the 'independent set of multiple binding sites' model.

To characterize changes in protein surface hydrophobicity, 8-anilino-1-naphthalenesulfonic acid (ANS) from Molecular Probes was used. In a 1ml quartz cuvette of cross section 5mm X 5mm, 10µM protein was mixed with 50µM ANS. Fluorescence measurements were conducted on a Horiba Jobin Yvon (HJY) Fluoromax 3 spectrofluorimeter (JOBIN YVON-SPEX). The excitation wavelength for ANS was 350 nm. The excitation and emission bandwidths were set at 5 nm. Spectral scan was carried out from 400 to 600 nm. The effect of Ca^{2+} or Mg^{2+} on the EfhP-ANS fluorescence was determined by adding $CaCl_2$ or $MgCl_2$ prepared in HEPES buffer to the cuvette. Spectra were collected for each Ca^{2+} or Mg^{2+} concentration from 10 to 100µM. As controls, spectra HEPES buffer alone and for 50µM ANS in HEPES were collected. Maximum fluorescence Intensity of the EfhP + ANS mixture was subtracted from maximum fluorescence intensities measured at different Ca^{2+} or Mg^{2+} concentrations. These differences were plotted against the Ca^{2+} concentration. Similar experiment was carried out with the mutant protein EFhPD88N. All the measurements were done using 10 µM protein and 50µM ANS, 20mM HEPES, 100mM NaCl at pH 7.

Replacing amino acids by site directed mutagenesis

Inverse PCR was used to generate point mutation D88N, shown in Figure 3.

Figure 3. This BLAST of the translation of the retrieved DNA with PA4107_NO_TM shows the mutation D88N in EfhP is made by the point mutation G305A.

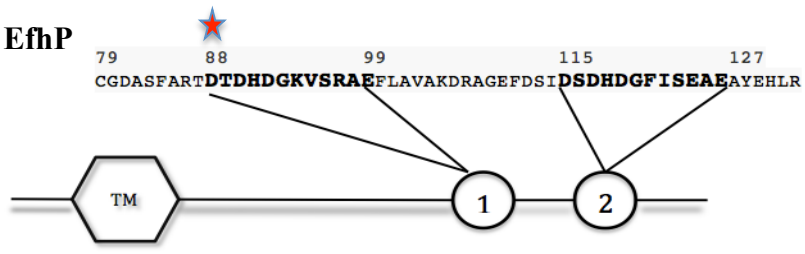

Figure 4. EfhP is shown with amino acid sequences of both EF-hands. The red star shows the location of the mutation made in EfhP_D88N.

Primers PA4017_D1N forward and reverse, shown in Table 1, containing the desired mutation were designed, and the vector containing the mutated gene was generated by using inverse PCR with the expression vector containing the wild-type No-TM-EfhP as the template. The PCR mixture contained 10µL DreamTaq Green PCR Master Mix, 1.5µL 2.5mM dNTPs (extra), 1µL forward primer, 1µL reverse primer, 1µL DNA template, and 5.5µL dH_2O for a total 20µL of reaction mixture. The denaturation step was programed to run at 95°C for 30 seconds, and the annealing step was programed to run at 56°C for 30 seconds. To enable amplification of the entire vector, the elongation phase of the reaction was programed to run for 2 minutes, (1 minute longer than usual), at 72°C . The reaction was only run for 19 cycles. To eliminate the original template, the PCR product received 1µL of the restriction enzyme DpnI and incubated in a 37°C water bath for 6 hours. Sufficient incubation time and amount of enzyme was established by observing no transformants after digesting template pDAV under the conditions mentioned above then heat shocking the digested plasmid into *E. coli*. The digested product was then transformed into heat shock competent DH5α *E. coli* cells using the protocol described above. Successful transformants were selected on agar plates with 50ng/µL kanamycin and confirmed by DNA sequencing. Once confirmed, the mutated soluble EfhP, EfhP_D88N was purified using His-tag affinity as described above.

Table 1.

Primer Name	Primer Sequences	Primer Function
efhP_OM/efhP	F: AGA GAG CAT ATG GAG CCG CTG GGC CAG R: AGA GAG GGA TCC TCA GTG CTG GCC TTG	Used to amplify the predicted cytoplasmic portion of *efhP* for heterologous expression and purification of EfhP
PA4107_D1N	F: GAC GCC TCC TTT GCC CGA ACC AAC ACC GAT CAC CAT GGC R: GCC ATC GTG ATC GGT GTT GGT TCG GGC AAA GGA GGC GTC	Used to make point mutation to generate mutant EfhP_D88N
PA4107_UP	F: TAA GCA CTC GAG GCC AGG TGG CTG TC R: TAA GCA GGA TCC GCT TCT TCT CCA CAG	Used to amplify the intergenic region upstream of *efhP* in order to generate promoter construct

Promoter activity construct and assays

To study the transcriptional regulation of *efhP,* a promoter construct pREN was generated by cloning the intergenic region upstream of *efhP* into the vector pCTX-1-lux between restriction sites for BamHI and XhoI, upstream of the promoterless *lux* operon, shown in Figure 5.

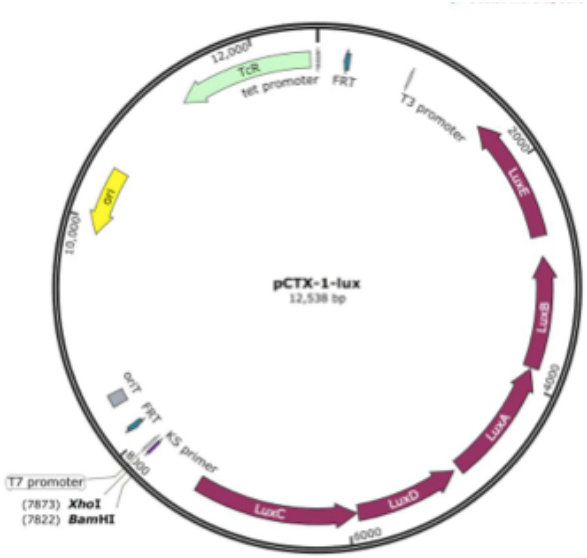

Figure 5. pCTX-1-lux is an integrase plasmid featuring the *lux* operon that will produce luminescence upon induction.

First, the intergenic region containing predicted promoter sequence upstream of the gene was amplified by PCR using the primers PA4107_UP forward and reverse, shown in Table 1. The amplified intergenic region and the vector pCTX-1-lux were digested using restriction enzymes BamHI and XhoI for 3 hours at 37°C. The promoter sequence was then cloned into pCTX-1-lux using a Quick Ligation kit (NEB). The ligation mixture containing 5µL vector and 4µL insert was incubated at room temperature for 15 minutes. For transformation, the ligation mixture was added to heat shock competent DH5α *E. coli* cells and transformed using the protocol described above. The successful transformants were selected on LB agar plates containing 20ng/µL tetracycline.

Once the promoter construct pREN was confirmed by DNA sequencing, it was transformed into PAO1 by electroporation [21]. For this, PAO1 was grown in LB broth at 37°C shaking overnight. The cells from 1.5mL culture were pelleted in microcentrifuge tubes and washed 3 times with 300mM sucrose, starting with 1mL and decreasing the volume by half with each wash. pREN was then added to the competent cells, mixed, and exposed to 1 pulse of electric shock (setting #2) of a BioRad electroporator. The cells were then transferred to glass tubes containing 1mL SOC and incubated for 2 hours shaking at 37°C. 150µL of the culture was then plated onto LB agar + 60mg/mL tetracycline. Successful transformants were screened by measuring increased luminescence.

Empty pCTX-1-lux was transformed into PAO1 to be used as a control using di-parental mating [22]. For this, donor SM10 *E. coli* cells containing the empty vector as well as the recipient PAO1 cells were grown in LB broth overnight at 37°C shaking. 1mL of the PAO1 culture was incubated at 42°C for 2 hours while 50µL of the SM10 cells were spot dried onto LB agar. 100µL of the PAO1 cells were spot dried directly on top of the *E. coli*. The mating mixture was then incubated at 37°C overnight. The following day, the mixed cells were resuspended in PBS and 50µL was spread onto PIA agar + 60mg/mL tetracycline.

To study the role of two component transcriptional regulators in regulating transcription of *efhP*, the pREN was also transformed into mutant strains lacking *bfmRS* and *carR* using the

mating protocol described above. Promoter activity assays were conducted using a Biotek 96-well plate reader. To prepare inoculum, 3mL cultures of the desired strains were grown in BMM for 12 hours. The ODs were normalized to 0.3 by diluting cultures in BMM. 10µL of the normalized culture was mixed with 990µL of BMM containing 0, 1, 3, 5, and 10mM Ca^{2+}. A white, flat-bottomed 96-well plate was inoculated with 100µL of each culture in 5 replicates. The plate was then incubated in the Biotek 96-well plate reader at 37°C shaking on the fast setting. Luminescence and absorbance at 600nm were measured every 30 minutes for 24 hours. Luminescence measurements were normalized by Ab_{600} of the corresponding cultures, followed by subtraction of the empty vector normalized luminescence. Finally, ratios between promoter activities determined with and without Ca^{2+} were calculated and averaged over at least three biological replicates. Every experiment was repeated at least twice.

RESULTS AND DISCUSSION

Heterologous expression and purification of EfhP

In order to avoid protein aggregation, to purify EfhP, only the portion of the gene encoding the predicted cytoplasmic part of the protein was cloned into the vector pET15b. The latter features ampicillin resistance marker for antibiotic selection as well as a TEV protease cleavage site used for cleaving the His-tag. The resulting construct pDAV is shown in Figure 6.

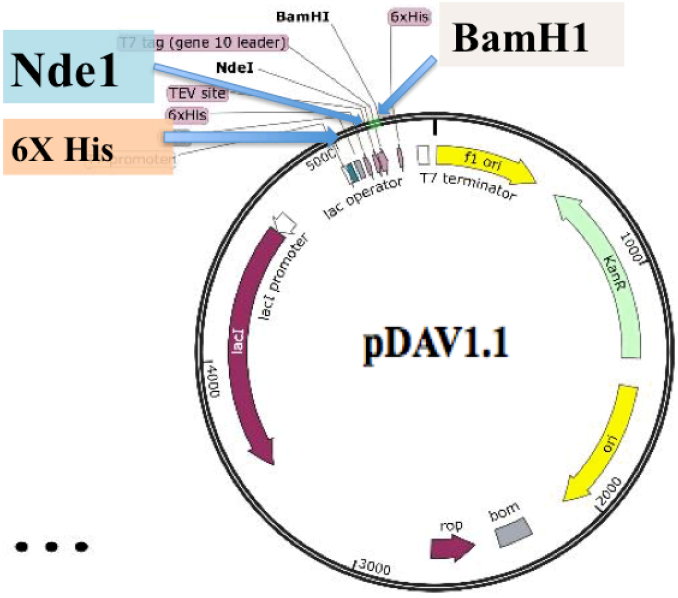

Figure 6. The construct pDAV was generated by cloning *efhP* into pET15b.

Following purification, the purified protein was confirmed as EfhP by SDS-PAGE and MALDI-TOF mass spectrometry. The image of the SDS-PAGE gel with estimated sizes of the purified EfhP before and after TEV digestion are shown in Figure 7.

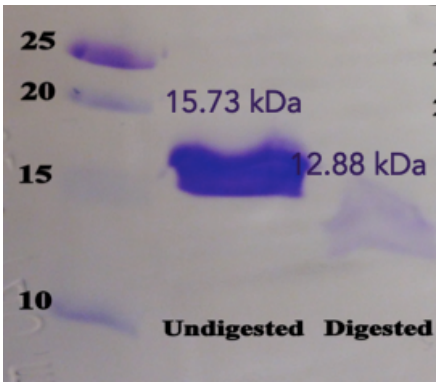

Figure 7. Molecular weight of the protein samples was estimated by SDS-PAGE. The undigested protein contained His-tags used for purification. The digested sample was treated with TEV to remove His-tags.

A monomeric form of EfhP was needed to study Ca^{2+}-binding and to characterize the kinetics of this binding. As shown in Figure 8, size exclusion chromatography was used to collect a monomeric fraction of the purified protein sample for further analyses.

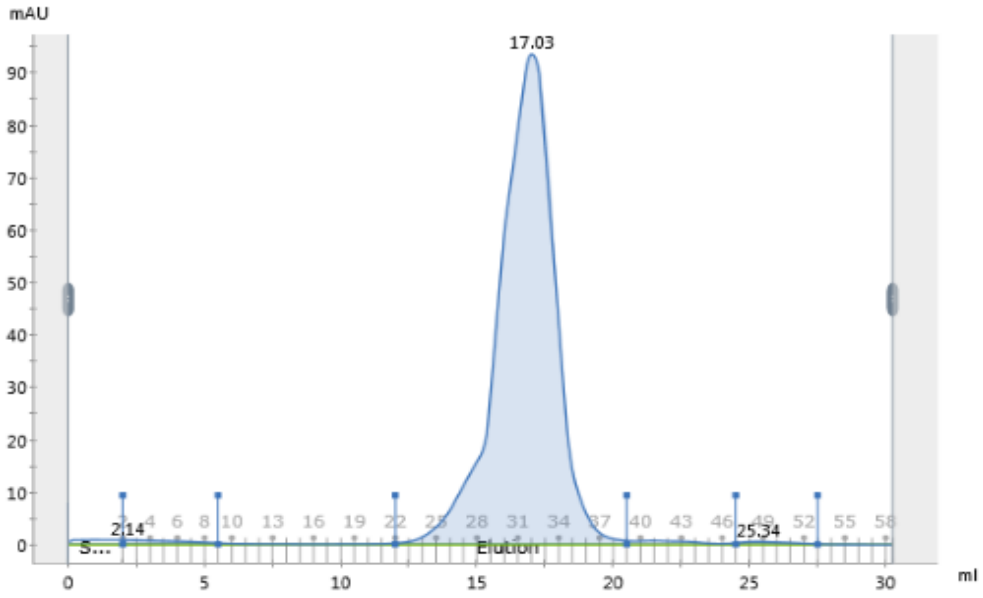

Figure 8. Size exclusion chromatography data for EfhP shows a single, monomeric peak.

Measuring EfhP Ca^{2+}-Binding:

The Ca^{2+}-binding capabilities of EfhP were measured by ITC. A titration curve resulting from addition of aliquots of 250µL 1mM Ca^{2+} to EfhP_NO_TM is shown in Figure 9.

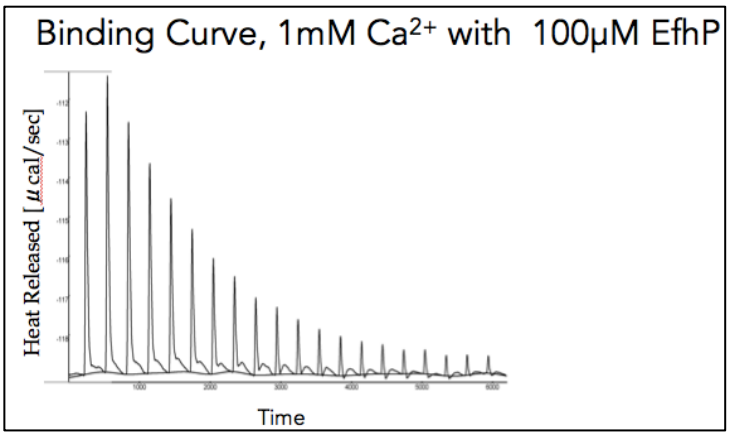

Figure 9. Measurements of heat released by the binding of Ca^{2+} by Efhp over time were used to calculate a binding constant that shows EfhP's strong affinity for Ca^{2+}.

The curve was fit to the 'independent set of multiple binding sites' model using the Bindworks software, which revealed an exothermic nature of the binding reaction. The binding enthalpy (Δ H) was -43.7KJ/mol, while the dissociation constant (Kd) was 18.2µM. A titration curve resulting from addition of aliquots of Mg^{2+} to EfhP_NO_TM is shown in Figure 5. For Mg^{2+}, the binding enthalpy (Δ H) of -0.24 KJ/mol. The heat generated by EfhP_NO_TM-Mg^{2+} is significantly lower than that generated by EfhP_NO_TM-Ca^{2+}, which supports the hypothesis that EfhP_NO_TM specifically binds Ca^{2+} but not Mg^{2+}. The high affinity and specificity of EfhP-Ca^{2+} binding support our hypothesis that EfhP functions as a Ca^{2+}-binding sensor in a Ca^{2+}-signaling pathway.

The EF-hand containing eukaryotic protein calmodulin (CaM) is known to bind to Ca^{2+} with Kd ranging from 10nM to 800µM [23] [24] [25]. Other eukaryotic EF hand proteins including secretagogin, a redox responsive Ca^{2+}-sensor, and Ca^{2+}-dependent protein kinases (CDPKs) were shown to have Kd values as low as 1µM and 5µM, respectively, indicating fairly high affinity Ca^{2+}-binding [26][24]. It is noteworthy that CaM, secretagogin and CDPKs function as Ca^{2+}-sensors. Cytosolic Ca^{2+} buffers like calbindin-D9k (CB-D9k), calbindin-D28k (CB-D28k), parvalbumins and calretinin (CR) have Ca^{2+} dissociation constants that are in low

micromolar ranges (0.2- 1.5μM) and unlike the sensors do not undergo conformational changes but help to spatiotemporally regulate cytosolic Ca^{2+} signals [28]. Considering the broad range of Ca^{2+} affinities among Ca^{2+}-binding proteins with different function, it is difficult to predict what role EfhP plays in a cell based on its Kd. However, taking into account that the intracellular level of Ca^{2+} in *P. aeruginosa* is about 0.1 μM, which increases to about 2-4 μM in response to elevated extracellular Ca^{2+} [19], and 1000 fold higher levels of Ca^{2+} in the periplasm as measured in *E. coli* [18]. Calmodulin has been shown to have Kd values as large as 10^4 μM indicating poor affinity [29]. In the present study we have observed very low heat generation from the binding of EfhP to Mg^{2+} that supports the expectation that EfhP selectively binds to Ca^{2+}.

Measuring Ca^{2+} induced changes in conformation of EfhP:

Based on the homology of EfhP to eukaryotic calmodulin, we predicted that Ca^{2+}-binding will lead to its conformational changes increasing hydrophobicity of the protein further enabling its Ca^{2+}-dependent interactions with protein targets. Depending on the nature of the targets, this interaction is expected to activate their activity and thus transduce the Ca^{2+} signal. To characterize Ca^{2+}-dependent hydrophobicity of EfhP, we measured the fluorescence of protein-ANS complex in response to addition of either Ca^{2+} or Mg^{2+}. The fluorescence of EfhP_NO_TM-ANS complex increased with increasing concentrations of Ca^{2+} up to 40μM Ca^{2+} (Fig.8). However, such increase was not observed with increasing concentrations of Mg^{2+} (Fig. 9). This supports the hypothesis that upon Ca^{2+}-binding, EfhP undergoes conformational changes that lead to increase in hydrophobicity. Further studies will aim to identify the targets of EfhP and their role in Ca^{2+} regulation.

Replacing amino acids by site directed mutagenesis

Based on the knowledge that the mutations of the first residue of the EF hand impairs Ca^{2+}-affinity in calmodulin, cardiac and skeletal troponin C, and myosin regulatory light chain, we predicted that mutating the D88N residue in EfhP would significantly reduce its Ca^{2+}-binding

[30]-[33]. Therefore we used site directed mutagenesis to obtain a mutant protein with impaired, if not abolished Ca^{2+}-binding abilities. These experiments aim to not only identify the Ca^{2+}-binding amino acids in EfhP, but enable generating a mutated EfhP for further functional studies. Since earlier studies showed thay EfhP regulates Ca^{2+}-dependent virulence in *P. aeruginosa* [20], we hypothesise this role of EfhP requires its ability to bind Ca^{2+}. To prove this hypothesis, we plan to test Ca^{2+}-dependent virulence factors in the *efhP* deletion mutant expressing the mutant EfhPD88N.

The mutant protein EfhP_D88N was obtained by an inverse PCR of the gene carrying vector and making a point mutation changing one nucleotide from G to A, which replaced an aspartic acid with an asparagine in the first EF-Hand, as shown previously in Figure 3. The mutant protein was purified and visualized using SDS-PAGE, as shown in Figure 10.

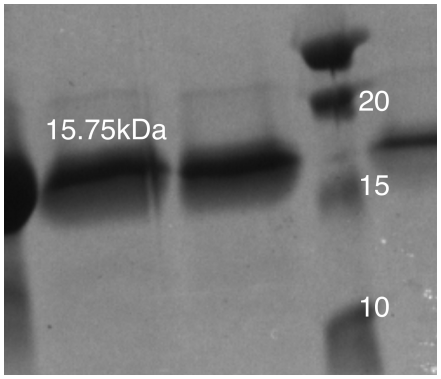

Figure 10. The purification of mutant EfhP was visualized using SDS-PAGE. The expected size of the mutant protein was 15.75kDA with His-tags still attached.

Measuring Ca^{2+}-binding and Ca^{2+} induced changes in conformation of the mutated EfhP_D88N:

To determine whether the mutation affected the ability of the mutated protein EfhP_D88N to bind Ca^{2+}, the protein was purified and subjected to ITC measurements. Titrating with Ca^{2+} revealed that EfhP_D88N has a Kd value of 62.61μM for Ca^{2+}, which is 3 folds higher than that for the wild-type protein (18.33μM). The titration curve for EfhP_D88N is shown in Figure 13. This higher Kd of the mutant protein implies a decrease in Ca^{2+} affinity. This shows that the first D of the first EF-hand loop has an important role in coordinating Ca^{2+} ion in the loop.

In order to study whether the mutant protein EfhP_D88N undergoes conformational changes induced by Ca^{2+}, we measured the fluorescence of protein-ANS complex in response to addition of either Ca^{2+} or Mg^{2+} and compared to the wild-type EfhP. The increase in fluorescence of the mutant protein EfhPD88N-ANS complex in response to adding Ca^{2+} was reduced in comparison to the wildtype protein. This proves that the first Aspartate (D) of the Ca^{2+}-binding loop of the first EF hand is important for Ca^{2+}-dependent structural rearrangements in the protein.

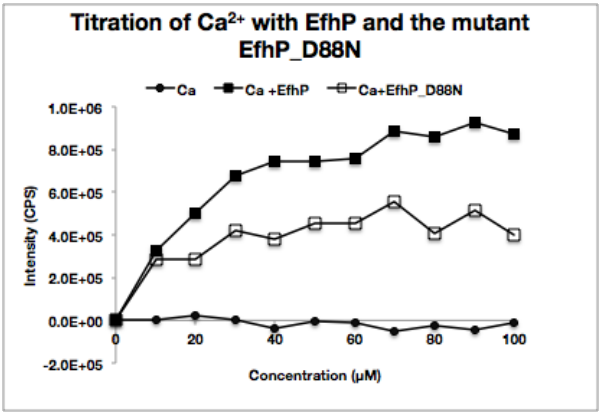

Figure 11. ANS analysis of EfhP and mutant EfhP_D88N in response to Ca^{2+}

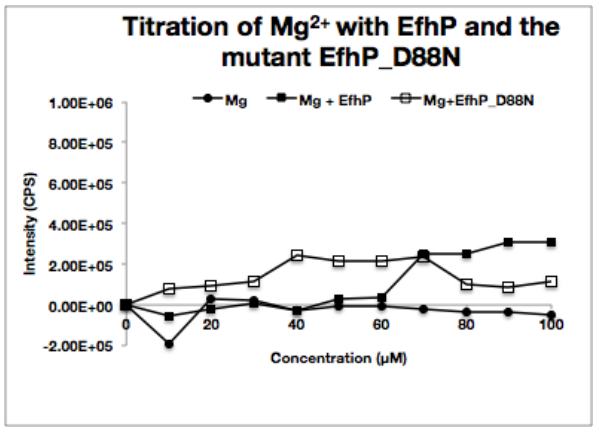

Figure 12. ANS analysis of EfhP and mutant EfhP_D88N in response to Mg^{2+}

Binding Curve, 1mM Ca^{2+} with 100µM EfhP_D88N

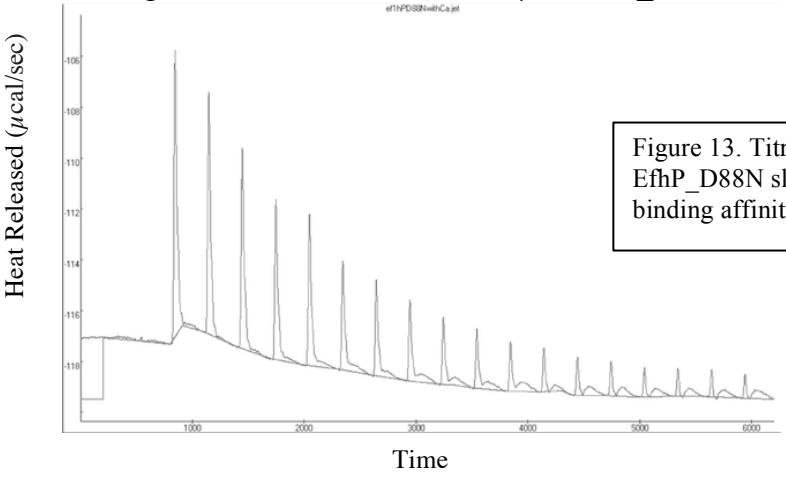

Figure 13. Titration curve for mutant protein EfhP_D88N shows a significant decrease in Ca^{2+}-binding affinity compared to wild-type EfhP.

Promoter activity construct and assays

To identify the environmental factors controlling transcription of *efhP,* we generated promoter activity constructs. Promoter activity assays are being conducted to study the effects of extracellular Ca^{2+} levels on the transcription of *efhP*. The promoter construct pREN, an integrase plasmid, has been transformed into the wildtype *P. aeruginosa* strain PAO1, which will be grown in a variety of Ca^{2+} concentrations. The luminescence measured in these assays will show the transcriptional effects of environmental Ca^{2+}. Similar assays will be conducted to investigate the effects of low iron, and elevated CO_2. The results of these experiments will reveal what environmental factors play a role in regulating the transcription of *efhP*.

Further studies are necessary to identify the partner proteins of EfhP cascading Ca^{2+}-signaling towards Ca^{2+}-dependent processes. Obtaining the knowledge about this signaling pathway will generate an insight into Ca^{2+}-signaling mechanisms in prokaryotes, which are currently not well known. This knowledge will provide a better understanding of the pathogenicity of bacteria such as *P. aeruginosa*, and will hopefully lead to the development of more successful treatment methods decreasing *P. aeruginosa* virulence and preventing its infections.

CONCLUSIONS

In the earlier studies, EfhP was shown to play a role in Ca^{2+}-induced virulence in human pathogen *P. aeruginosa*. Here we provided an experimental confirmation that EfhP selectively binds Ca^{2+}. We also measured the affinity of the binding, and the elucidated Kd supports the hypothesis of the cytoplasmic localization of the EF hands of the protein. Furthermore, we have determined the role of the 1^{st} D in the 1^{st} EF hand in Ca^{2+}-binding. We also showed that EfhP increased its hydrophobicity upon Ca^{2+}-binding, and that decreased Ca^{2+}-binding decreases such structural rearrangements. This suggests that binding Ca^{2+} increases the ability of the protein to interact with other proteins. These findings provide the foundation for further studies aiming to determine whether Ca^{2+}-binding is essential to EfhP function in *P. aeruginosa* virulence.

Finally, we have generated a genetic construct to identify the environmental factors contributing to the regulation of transcription of *efhP*. By identifying the host factors regulating *efhP* transcription, we will gain a better understanding of how to inhibit this protein's function. The data obtained from these experiments will further characterize the role of EfhP in Ca^{2+} signaling pathways. Further analysis of this protein is needed for the development of targeted treatments aiming to decrease *P. aeruginosa* virulence and prevent the severe infections by this pathogen.

REFERENCES

1. Falagas ME, Bliziotis IA (2007) Pandrug-resistant Gram-negative bacteria: the dawn of the post-antibiotic era? International journal of antimicrobial agents 29: 630–636.
2. Kaye KS, Kanafani ZA, Dodds AE, Engemann JJ, Weber SG, et al. (2006) Differential effects of levofloxacin and ciprofloxacin on the risk for isolation of quinolone-resistant Pseudomonas aeruginosa. Antimicrobial agents and chemotherapy 50: 2192–2196.
3. Bicanic TA, Eykyn SJ (2002) Hospital-acquired, native valve endocarditis caused by Pseudomonas aeruginosa. The Journal of infection 44: 137–139.
4. Ishiwada N, Niwa K, Tateno S, Yoshinaga M, Terai M, et al. (2005) Causative organism influences clinical profile and outcome of infective endocarditis in pediatric patients and adults with congenital heart disease. Circulation journal 69: 1266–1270.
5. Komshian SV, Tablan OC, Palutke W, Reyes MP (1990) Characteristics of left-sided endocarditis due to Pseudomonas aeruginosa in the Detroit Medical Center. Reviews of infectious diseases 12: 693–702.
6. Jesaitis AJ, Franklin MJ, Berglund D, Sasaki M, Lord CI, et al. (2003) Compromised host defense on Pseudomonas aeruginosa biofilms: characterization of neutrophil and biofilm interactions. J Immunol 171: 4329–4339.
7. Walters MC 3rd, Roe F, Bugnicourt A, Franklin MJ, Stewart PS (2003) Contributions of antibiotic penetration, oxygen limitation, and low metabolic activity to tolerance of Pseudomonas aeruginosa biofilms to ciprofloxacin and tobramycin. Antimicrob Agents Chemother 47: 317–323.
8. Carafoli E (2002) Calcium signaling: a tale for all seasons. Proceedings of the National Academy of Sciences of the United States of America 99: 1115–1122.
9. von Ruecker AA, Bertele R, Harms HK (1984) Calcium metabolism and cystic fibrosis: mitochondrial abnormalities suggest a modification of the mitochondrial membrane. Pediatric research 18: 594–599.
10. Lorin MI, Gaerlan PF, Mandel ID, Denning CR (1976) Composition of nasal secretion in patients with cystic fibrosis. The Journal of laboratory and clinical medicine 88: 114–117.
11. Halmerbauer G, Arri S, Schierl M, Strauch E, Koller DY (2000) The relationship of eosinophil granule proteins to ions in the sputum of patients with cystic fibrosis. Clinical and experimental allergy 30: 1771–1776.
12. Dominguez DC (2004) Calcium signalling in bacteria. Molecular microbiology 54: 291–297.
13. Herbaud ML, Guiseppi A, Denizot F, Haiech J, Kilhoffer MC (1998) Calcium signalling in Bacillus subtilis. Biochimica et biophysica acta 1448: 212–226.
14. Borriello G, Werner E, Roe F, Kim AM, Ehrlich GD, et al. (2004) Oxygen limitation contributes to antibiotic tolerance of Pseudomonas aeruginosa in biofilms. Antimicrob Agents Chemother 48: 2659–2664.
15. Leganes F, Forchhammer K, Fernandez-Pinas F (2009) Role of calcium in acclimation of the cyanobacterium Synechococcus elongatus PCC 7942 to nitrogen starvation. Microbiology 155: 25–34.
16. Zhao Y, Shi Y, Zhao W, Huang X, Wang D, et al. (2005) CcbP, a calcium-binding protein from Anabaena sp. PCC 7120, provides evidence that calcium ions regulate

heterocyst differentiation. Proc Natl Acad Sci U S A 102: 5744–5748.

17. Leganes F, Forchhammer K, Fernandez-Pinas F (2009) Role of calcium in acclimation of the cyanobacterium *Synechococcus elongatus* PCC 7942 to nitrogen starvation. Microbiology-Sgm 155: 25–34.
18. Campbell AK, Naseern R, Holland IB, Matthews SB, Wann KT (2007) Methylglyoxal and other carbohydrate metabolites induce lanthanum-sensitive Ca^{2+} transients and inhibit growth in *E.coli*. Archives of Biochemistry and Biophysics 468: 107–113.
19. Guragain M, Lenaburg DL, Moore FS, Reutlinger I, Patrauchan MA (2013) Calcium homeostasis in Pseudomonas aeruginosa requires multiple transporters and modulates swarming motility. Cell Calcium 54: 350–361.
20. Sarkisova SA, Lotlikar SR, Guragain M, Kubat R, Cloud J, Franklin MJ, et al. (2014) A *Pseudomonas aeruginosa* EF-Hand Protein, EfhP (PA4107), Modulates Stress Responses and Virulence at High Calcium Concentration. PLoS ONE 9(6): e98985. https://doi.org/10.1371/journal.pone.0098985
21. Dr. M.A. Patrauchan lab electroporation protocol
22. Dr. M.A. Patrauchan lab mating protocol
23. Ikura, Mitsuhiko. "Calcium binding and conformational response in EF-hand proteins." *Trends in biochemical sciences* 21.1 (1996): 14-17.
24. Mella, Manuela. "Molecular mechanism of the Ca2+-dependent activation of sorcin (soluble resistance-related calcium binding protein. A study with site-specific mutants." (2007).
25. Cox, Jos A. "Divers models of divalent cation interaction to calcium-binding proteins: techniques and anthology." *Calcium-Binding Proteins and RAGE*. Humana Press, Totowa, NJ, 2013. 15-35.
26. Bauer, Mikael C., et al. "Identification of a high-affinity network of secretagogin-binding proteins involved in vesicle secretion." *Molecular BioSystems* 7.7 (2011): 2196-2204.
27. Ying, Sheng, et al. "Regulatory Phosphorylation of Bacterial-type PEP Carboxylase by the Ricinus kinase CDPK1." *Plant physiology* (2017): pp-00288.
28. Schwaller, Beat. "Cytosolic Ca2+ buffers." *Cold Spring Harbor perspectives in biology* 2.11 (2010): a004051.
29. Cox, Jos A., et al. "Mode of action of the regulatory protein calmodulin." *Metal ions in biological systems* 17 (1984): 215-273.
30. Putkey, John A., H. Lee Sweeney, and S. T. Campbell. "Site-directed mutation of the trigger calcium-binding sites in cardiac troponin C." *Journal of Biological Chemistry* 264.21 (1989): 12370-12378
31. Sheng, Zelin, et al. "Evidence that both Ca (2+)-specific sites of skeletal muscle TnC are required for full activity." *Journal of Biological Chemistry* 265.35 (1990): 21554-21560.
32. Reinach, Fernando C., Kiyoshi Nagai, and John Kendrick-Jones. "Site-directed mutagenesis of the regulatory light-chain Ca2+/Mg2+ binding site and its role in hybrid myosins." *Nature*322.6074 (1986): 80
33. Xiong, Liang-Wen, et al. "Intra-and interdomain effects due to mutation of calcium-binding sites in calmodulin." *Journal of Biological Chemistry* 285.11 (2010): 8094-8103.